

Channel-Adaptive Wireless Image Transmission with OFDM

Haotian Wu, Yulin Shao, Krystian Mikolajczyk, and Deniz Gündüz

Department of Electrical and Electronic Engineering, Imperial College London, London SW7 2BT, UK

Email: {haotian.wu17, y.shao, k.mikolajczyk, d.gunduz} @imperial.ac.uk

Abstract—We present a learning-based channel-adaptive joint source and channel coding (CA-JSCC) scheme for wireless image transmission over multipath fading channels. The proposed method is an end-to-end autoencoder architecture with a dual-attention mechanism employing orthogonal frequency division multiplexing (OFDM) transmission. Unlike the previous works, our approach is adaptive to channel-gain and noise-power variations by exploiting the estimated channel state information (CSI). Specifically, with the proposed dual-attention mechanism, our model can learn to map the features and allocate transmission-power resources judiciously based on the estimated CSI. Extensive numerical experiments verify that CA-JSCC achieves state-of-the-art performance among existing JSCC schemes. In addition, CA-JSCC is robust to varying channel conditions and can better exploit the limited channel resources by transmitting critical features over better subchannels.

Index Terms—Joint source channel coding, deep neural networks, OFDM, image communications.

I. INTRODUCTION

Shannon’s separation theorem states that it is optimal to design source and channel coding separately in the asymptotic limit of infinite block-length [1]. However, this implicitly assumes unlimited delay and complexity, which does not hold in practice. An increasing number of wireless applications, such as Internet-of-things and edge intelligence [2]–[5], require efficient transmission of large volumes of data under strict delay constraints. This resulted in an increasing interest in joint source channel coding (JSCC) scheme in recent years. Earlier works on JSCC focused on theoretical analysis with ideal source and channel distributions [6], [7], or jointly optimizing the parameters of separately designed source and channel coding blocks [8], [9]. Recently, however, inspired by the impressive performance of deep learning techniques in computer vision and natural language processing applications, researchers have started to exploit deep neural networks to design novel and competitive JSCC schemes to transmit high information content signals, such as images or videos, over wireless channels [10]–[17].

This approach has been pioneered in [10], where an autoencoder-based JSCC architecture is proposed for wireless image transmission, which outperformed state-of-the-art conventional compression and channel coding schemes over additive white Gaussian noise (AWGN) and Rayleigh fading channels. This was later extended to feedback channels in [11] and to bandwidth-adaptive transmission in [18]. In [13],

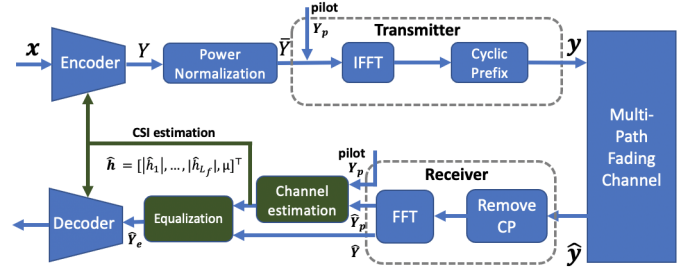


Fig. 1: Our proposed channel-adaptive CA-JSCC scheme.

authors consider JSCC over orthogonal frequency division multiplexing (OFDM) channels. These deep learning aided JSCC scheme are shown to outperform conventional schemes with separate source and channel coding techniques. Superiority of the JSCC approach was recently extended to video transmission in [17]. An alternative variational autoencoder architecture is also considered in [14]–[16].

However, adaptivity to channel conditions is still a challenge for deep learning based JSCC. Methods in [10], [11], [18] are either trained for a specific signal-to-noise ratio (SNR), or the neural network parameters are trained and used for a wide range of channel SNRs. The former requires significant storage memory as different network parameters need to be stored and used in different channel conditions, where the latter sacrifices performance and cannot exploit the channel state information (CSI) often available in communication systems. In conventional digital communication systems, CSI at the encoder can allow power allocation to boost the communication rate. In [13], [19], CSI is used in a similar manner, mainly to adjust the feature weights according to channel state; however, in the case of OFDM, CSI will be instrumental not only for power control, but also to decide in mapping the features to different subcarriers according to their relative qualities. For example, more critical features of the input image can be mapped to more reliable channels. We introduce a channel-adaptive JSCC (CA-JSCC) scheme, which employs a dual-attention mechanism to adjust its network parameters according to the estimated CSI at the encoder and decoder.

Our dual-attention mechanism consists of *channel-wise* attention learning and *spatial* attention learning, which learns to map the features and allocates power judiciously in the multi-scale intermediate layers. Our method achieves state-of-

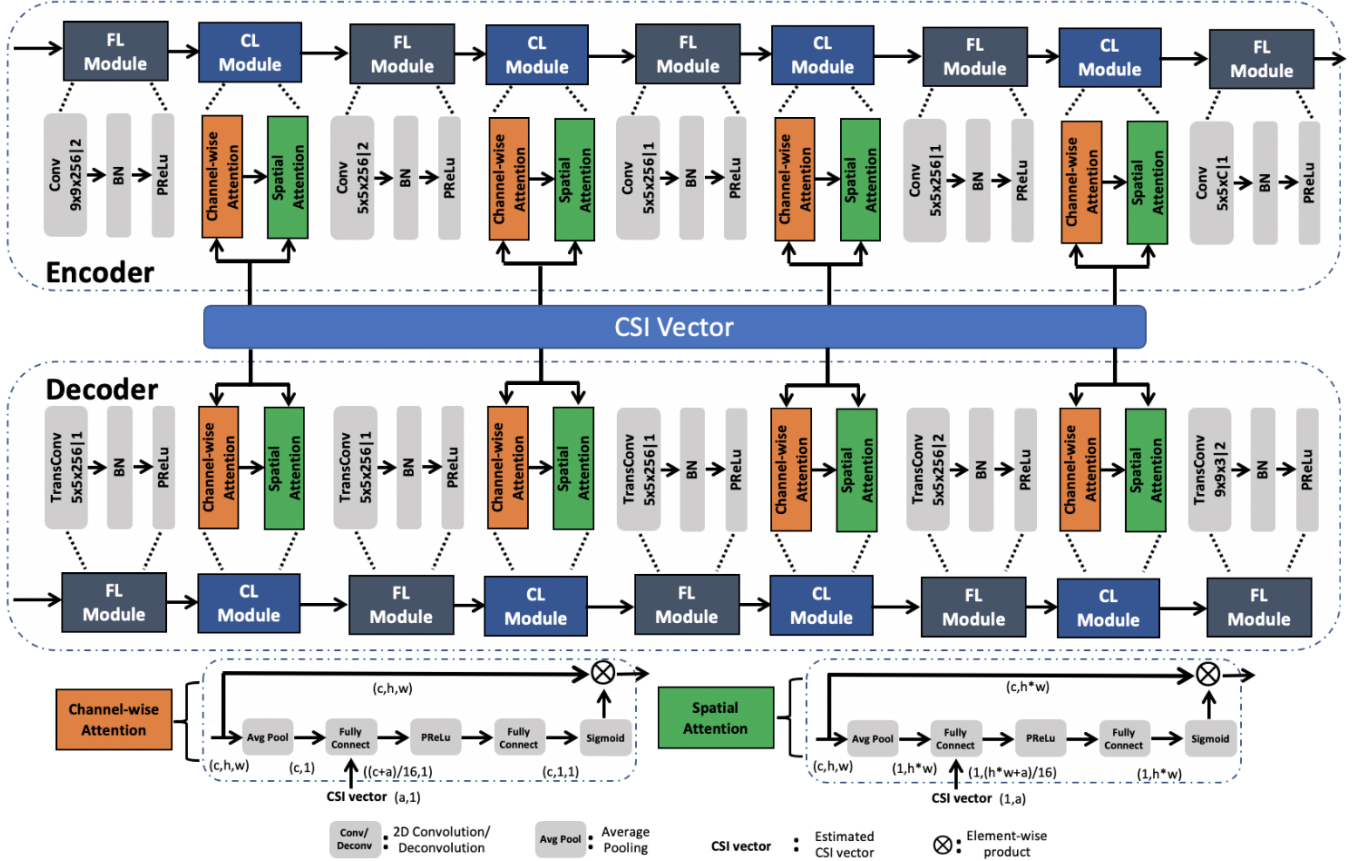


Fig. 2: Basic blocks of our dual-attention encoder and decoder architectures.

the-art performance and adapts to different SNR scenarios, making it unnecessary to retrain separate JSCC models for different channel conditions. Our method also helps JSCC simultaneously use the estimated CSI to allocate the power, making JSCC adaptive to all channel conditions.

II. SYSTEM MODEL

We consider the OFDM-based JSCC of images over a multipath fading channel with L_t paths. We transmit each input image using N_s OFDM symbols accompanied with N_p pilots for channel estimation, per OFDM subcarrier. As shown in Fig 1, an encoding function E_θ first maps the input image $\mathbf{x} \in \mathbb{R}^{c \times h \times w}$ into a complex matrix $\mathbf{Y} \in \mathbb{C}^{N_s \times L_f}$, where c, h and w denote the color, height and width of the image. The generated channel input can be denoted by $\mathbf{Y} = E_\theta(\mathbf{x}, \hat{\mathbf{h}})$, where $\hat{\mathbf{h}}$ is the estimated CSI vector available at the transmitter.

Channel input \mathbf{Y} is subject to an average power constraint $P_s: \frac{1}{N_s L_f} \mathbb{E}[\|\mathbf{Y}\|_F^2] \leq P_s$, where the expectation is taken over the input images, and $\|\cdot\|_F$ denotes the Frobenius norm. Without loss of generality, we set $P_s = 1$.

Each OFDM symbol is passed through the inverse discrete Fourier transform (IDFT) module, appended with the cyclic prefix (CP), and transmitted to the receiver over the multipath channel. The transfer function of the multipath fading channel

with L paths is defined as: $\hat{\mathbf{y}} = h_c(\mathbf{y}) = \mathbf{h}_t * \mathbf{y} + \mathbf{w}$, where \mathbf{y} and $\hat{\mathbf{y}}$ denote the input and output vectors, respectively; $*$ is the linear convolution operation, $\mathbf{h}_t \in \mathbb{C}^L$ is the channel impulse response, and \mathbf{w} is the AWGN term.

The receiver first demodulates $\hat{\mathbf{y}}$ by removing the CP and applying fast Fourier transform (FFT) operations. The equivalent frequency-domain transfer function of h_c can be written as:

$$\hat{\mathbf{Y}}[i, k] = H[k] \bar{\mathbf{Y}}[i, k] + W[i, k], \quad (1)$$

where the frequency-domain channel matrix $\mathbf{H} \in \mathbb{C}^{(L_f, L_f)}$ is a diagonal matrix with the k -th diagonal element being $H[k]$ (frequency-domain channel response of the k -th subcarrier). Let $\bar{\mathbf{Y}} \in \mathbb{C}^{(N_s, L_f)}$ denote the output of the power normalization module at the transmitter (i.e., the inputs to the IDFT module), where $\bar{\mathbf{Y}}[i, k]$ denotes the symbol at the k -th subcarrier of the i -th OFDM symbol. $\mathbf{W} \in \mathbb{C}^{(N_s, L_f)}$ is the frequency domain noise matrix, where $W[i, k] \sim \mathcal{CN}(0, \sigma^2)$ and independent of each other.

Given the FFT output of the pilots at the receiver, we use minimum mean square error (MMSE) or least square (LS) channel estimator to estimate the CSI ($H[k]$) in frequency-domain (Eqn. (1)). The estimated CSI vector $\hat{\mathbf{h}}$ can then be used to equalize the data (MMSE equalizer). We have

$$\hat{\mathbf{h}} \triangleq [|\hat{h}_1|, |\hat{h}_2|, \dots, |\hat{h}_{L_f}|, \mu]^T, \quad (2)$$

where \hat{h}_i , $i = 1, 2, \dots, L_f$, is the estimated channel gain of the i -th subcarrier; while μ is the signal-to-noise ratio (SNR) defined as $\mu = 10 \log_{10} \frac{P_s}{\sigma^2}$ dB for transmit power P_s and noise power σ^2 .

Based on the equalized data \hat{Y}_e and the estimated CSI vector $\hat{\mathbf{h}}$, the decoder D_ϕ reconstructs the transmitted image as $\hat{\mathbf{x}}$, i.e., $\hat{\mathbf{x}} = D_\phi(\hat{Y}_e, \hat{\mathbf{h}})$. The performance indicator is the peak signal-to-noise ratio (PSNR), defined as $\text{PSNR} = 10 \log_{10} \frac{(\max \mathbf{x})^2}{\text{MSE}(\mathbf{x}, \hat{\mathbf{x}})}$ (dB), where $\max \mathbf{x}$ denotes the maximum possible value of the input signal \mathbf{x} , $\text{MSE}(\mathbf{x}, \hat{\mathbf{x}}) \triangleq \|\mathbf{x} - \hat{\mathbf{x}}\|_2^2$.

We then jointly train the encoder and decoder to minimize the loss function $\mathcal{L}(\theta, \phi) = \mathbb{E}[\text{PSNR}(\mathbf{x}, \hat{\mathbf{x}})]$, where the expectation is taken over the randomness both in the source and channel distributions. We aim to find the optimal parameters (θ^*, ϕ^*) that minimize the expected loss $\mathcal{L}(\theta, \phi)$.

III. DUAL-ATTENTION MECHANISM

In OFDM systems, different subcarriers face different channel gains, and a judicious transmission scheme should be able to allocate power as well as features across appropriate subcarriers to adapt to channel variations. To fully exploit the estimated CSI, we propose a dual-attention based CA-JSCC scheme, which introduces the estimated CSI in multi-scale intermediate layers. The architecture of our method is shown in Fig 2.

As shown in Fig 2, both the encoder and the decoder have feature learning (FL) and channel learning (CL) modules. The FL module consisting of 2D convolution/deconvolution, batch normalization, and PRelu layers, is designed to directly learn an intermediate feature of the input. Following the FL module, the CL module learns to generate an attention mask to map features to appropriate subcarriers based on the estimated CSI and input features. The CL module is dual-attention based with a *channel-wise* attention module and a *spatial* attention module (*channel-wise* here refers to the channels of the feature maps). Its operation is presented in Algorithm 1.

1) *Channel-wise attention module*: Our *channel-wise* attention module is inspired by [19], which adapts to a single SNR value in an AWGN channel model. Instead, CA-JSCC learns an attention mask to allocate and map features based on the estimated CSI of all N_s subcarriers.

We first apply average pooling $\text{Ave}_c(\mathbf{F}_{in})$ on input features \mathbf{F}_{in} along the spatial direction to get vector \mathbf{F}_{ca} , where $\text{Ave}_c(\mathbf{F}_{in}) \triangleq \frac{1}{hw} \sum_{j=1}^h \sum_{k=1}^w \mathbf{F}_{in}[c, h, w]$. \mathbf{F}_{ca} is then concatenated with $\hat{\mathbf{h}}$ to get the intermediate vector \mathbf{i}_c to compute the *channel-wise* attention mask \mathbf{S}_c by several fully connected (FC) layers: $\mathbf{S}_c = f_c(\mathbf{i}_c)$, where f_c represents the FC layers followed by PReLU functions. Finally, we get the output of our *channel-wise* attention module as $\mathbf{F}_{cout} = \mathbf{S}_c \cdot \mathbf{F}_{in}$.

Our *channel-wise* attention module learns to map features from the input to the subcarriers based on the estimated CSI, allowing JSCC to dynamically adjust to different channel SNRs. But the spatial information is ignored when computing the channel attention mask by average pooling operation. So we design a *spatial* attention learning module to compensate for spatial information.

Algorithm 1 Dual-attention based CL

Input: $\mathbf{F}_{in} \in \mathbb{R}^{c \times h \times w}$, $\hat{\mathbf{h}} \in \mathbb{R}^{L_f+1}$

Output: $\mathbf{F}_{out} \in \mathbb{R}^{c \times h \times w}$

Stage 1: Channel-wise attention

- 1: $\mathbf{F}_{ca} = \text{Ave}_c(\mathbf{F}_{in}) \in \mathbb{R}^{(c)}$
- 2: $\mathbf{i}_c = \text{concatenate}(\mathbf{F}_{ca}, \hat{\mathbf{h}}) \in \mathbb{R}^{(c+L_f+1)}$
- 3: $\mathbf{S}_c = f_c(\mathbf{i}_c) \in \mathbb{R}^{(c,1,1)}$
- 4: **for** $i = 0:1:c$ **do**
- 5: $\mathbf{F}_{cout}[i, h, w] = \mathbf{S}_c[i] \cdot \mathbf{F}_{in}[i, h, w] \in \mathbb{R}^{(c,h,w)}$
- 6: **end for**

Stage 2: Spatial attention

- 1: $\mathbf{F}_{sa} = \text{Ave}_s(\mathbf{F}_{cout}) \in \mathbb{R}^{(1,h,w)} \Rightarrow \mathbb{R}^{(hw)}$
- 2: $\mathbf{i}_s = \text{concatenate}(\mathbf{F}_{sa}, \hat{\mathbf{h}}) \in \mathbb{R}^{(hw+L_f+1)}$
- 3: $\mathbf{S}_s = f_s(\mathbf{i}_s) \in \mathbb{R}^{(h,w)} \Rightarrow \mathbb{R}^{(h,w)}$
- 4: **for** $j = 0:1:h$ **do**
- 5: **for** $k = 0:1:w$ **do**
- 6: $\mathbf{F}_{out}[c, j, k] = \mathbf{S}_s[j, k] \cdot \mathbf{F}_{cout}[c, j, k] \in \mathbb{R}^{(c,h,w)}$
- 7: **end for**
- 8: **end for**

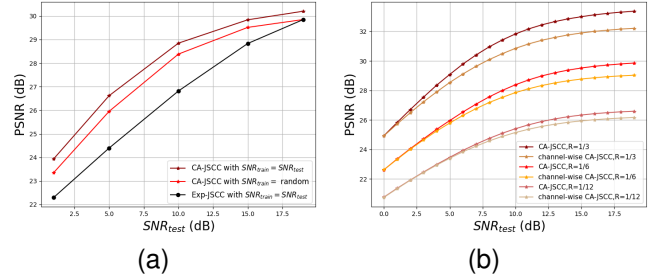


Fig. 3: (a) Comparison of the proposed CA-JSCC scheme with Exp-JSCC when the values of the train and test SNRs are the same. (b) Ablation experiments for the attention strategy.

2) *Spatial attention module*: Our *spatial* attention module learns to match the critical spatial features with better channel conditions depending on the estimated CSI.

We firstly apply average pooling operation $\text{Ave}_s(\mathbf{F}_{cout})$ on the \mathbf{F}_{cout} along the channel direction to get \mathbf{F}_{sa} , where $\text{Ave}_s(\mathbf{F}_{cout}) \triangleq \frac{1}{c} \sum_{j=1}^c \mathbf{F}_{cout}[c, h, w]$. Then, $\hat{\mathbf{h}}$ and \mathbf{F}_{sa} are concatenated to get the intermediate feature \mathbf{i}_s , which is used to compute the *spatial* mask \mathbf{S}_s by several FC layers. We compute the final output feature vector as $\mathbf{F}_{out} = \mathbf{S}_s \cdot \mathbf{F}_{cout}$.

This *spatial* attention module can further improve the PSNR performance by exploiting the spatial information and helping JSCC encoder do more adaptive power allocation, which matches critical features with better channels. That is, features that are more critical for the reconstruction of the input image are transmitted via better channels.

IV. TRAINING AND EVALUATION

This section presents numerical experiment results to evaluate the performance of our CA-JSCC scheme.

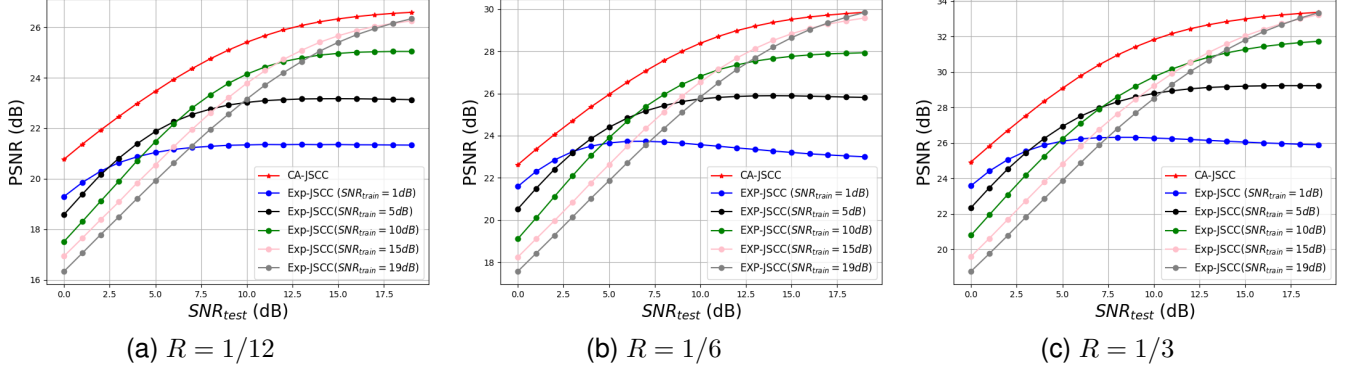


Fig. 4: Performance of our CA-JSCC model compared with the Exp-JSCC model of different bandwidth ratios.

A. Experimental setup

The experiments were performed on the CIFAR-10 dataset [20] with Pytorch. Models were trained until the performance of a validation set (selected and separated from the training dataset) stop improving. The Adam optimizer is used to perform backpropagation. The scheme with CSI introduced in [13] (denoted as EXP-JSCC) is used as the benchmark.

We set the number of subcarriers to $L_f = 64$. The Zadoff-Chu (ZC) sequence [21], denoted by $\mathbf{Y}_p \in \mathbb{C}^{(2,64)}$, is used as the pilot. The values of channel gains $\{H[k] : k = 1, 2, \dots, L_f\}$ are sampled from a complex Gaussian distribution $\mathcal{CN}(0, 1)$. If not specified otherwise, the frequency-domain channel responses in the experiments are estimated by the MMSE estimator. We also sort the channels based on their estimated CSI to make training process easier; that is, we have $|H[1]|^2 \geq \dots \geq |H[L]|^2$. Following [11], we define the bandwidth ratio (i.e., bandwidth usage to source symbol ratio) as $R \triangleq \frac{N_s L_f}{c \times h \times w}$, where $N_s L_f$ is the number of symbols transmitted per image.

B. Channel-gain adaptability

We first verify the adaptability of the CA-JSCC scheme to channel-gain variations. Specifically, under a fixed bandwidth ratio and a given SNR, we want to see if our dual-attention mechanism can instruct the transmitter to exploit better channels and allocate power to different subcarriers judiciously.

The experimental results are shown in Fig 3a, where we set the number of OFDM symbols to $N_s = 4$ and the bandwidth ratio to $R = 1/6$. The Exp-JSCC and CA-JSCC models are both trained at a fixed SNR, and tested at the same SNR. As can be seen, by feeding the estimated CSI to the transmitter, CA-JSCC can exploit the channel-gain information and adaptively allocate power to different subcarriers. We can see a significant gain compared to Exp-JSCC at all SNRs. This can be attributed to the advantage of our method in better exploiting the channel gains and allocating power to different subcarriers.

C. SNR adaptability

Next, we evaluate the SNR adaptability of our scheme. If not specified otherwise, we train the CA-JSCC model at random SNR values of each training episode chosen uniformly from the range $[0, 20]$ dB and test the well-trained model at different SNRs.

Compared with the CA-JSCC scheme trained at specific SNRs in Fig 3a, we observe that there is a slight performance deprecation when training the CA-JSCC at random SNR values. We conclude that, while CA-JSCC can learn to adapt to different channel SNRs, this flexibility comes at the expense of some loss in the PSNR (up to 0.7dB). However, this CA-JSCC model trained at random SNR values still outperforms the Exp-JSCC models trained at specific SNR values.

We also compare the performance of CA-JSCC with different attention strategies in the CL modules as an ablation study: dual-attention based CL and only channel-wise attention based CL. As shown in Fig 3b, for different bandwidth values, our dual-attention based CA-JSCC architecture outperforms channel-wise attention based CL module, which shows the effectiveness of our *spatial* attention mechanism. We also observe large gains by our dual-attention method for higher bandwidth ratios and SNR_{test} values, where more spatial information and better CSI adaptability benefit the feature mapping and power allocation. It is worth noting that the Exp-JSCC scheme is not SNR-adaptive, which means the training and test SNRs of Exp-JSCC must match to achieve a sound performance.

Fig 4 presents the PSNR versus test SNR results for bandwidth ratios of $R = 1/12, 1/6, 1/3$ (we set $L_f = 64$ and vary N_s to attain different R values). As stated above, our CA-JSCC scheme can be trained at a range of SNRs, and yields a single model for each bandwidth ratio to be verified on a range of test SNRs. The Exp-JSCC scheme, on the other hand, is trained at five different SNRs, yielding five different models under each bandwidth ratio. The Exp-JSCC scheme performs the best when the training and test SNRs match. However, our CA-JSCC scheme is SNR-adaptive

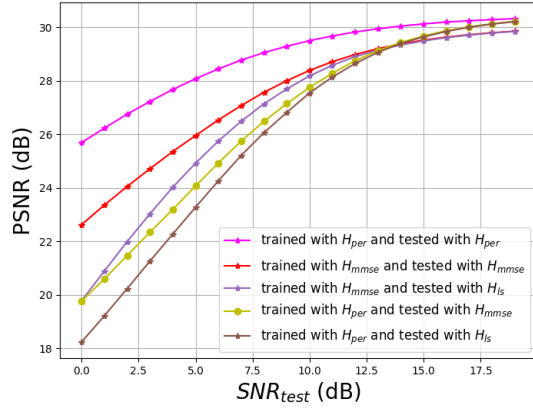


Fig. 5: Comparison of CA-JSCC with different channel estimation methods.

and consistently outperforms Exp-JSCC at all SNRs and bandwidth ratios with a considerable margin.

D. Impact of CSI estimation errors

In the above experiments, we have assumed MMSE estimated CSI. In this subsection, we look into the effect of channel estimation errors on the performance of CA-JSCC. We repeat the experiment in Fig 4b with three types of CSI: i) perfect CSI, H_{per} ; ii) MMSE estimated CSI, H_{mmse} ; and iii) LS estimated CSI, H_{ls} . H_{mmse} provides a more accurate estimate than H_{ls} .

The experimental results are shown in Fig 5, where we train our CA-JSCC models with H_{mmse} and H_{per} , respectively, and evaluate these two models with H_{per} , H_{mmse} and H_{ls} , respectively. As expected, the model trained and tested with H_{per} achieves the best performance. On the other hand, the model trained with perfect CSI is not robust to CSI errors during test time. Its performance gets worse as the quality of channel estimation degrades. Instead, we see that models trained with H_{mmse} perform better since they learn to compensate for CSI imperfections. We conclude from these results that a more accurate CSI during testing is generally beneficial, and the performance improves if training is done with the same type of CSI.

V. CONCLUSION

We presented the CA-JSCC scheme for wireless image transmission over OFDM channels. We proposed a dual-attention mechanism to simultaneously exploit the estimated CSI to aid the allocation of features and power resources adaptively. The dual-attention mechanism comprises a *channel-wise* attention module, which learns to map features to channels, and a *spatial* attention module, which learns high-level spatial features, allowing the JSCC encoder to match the most important features with the most reliable subcarriers. Numerical experiments show that our method achieves state-of-the-art performance in various SNR and bandwidth scenarios.

Besides, our method simultaneously uses the estimated CSI to adapt to time-varying channel conditions.

REFERENCES

- [1] C. E. Shannon, "A mathematical theory of communication," *The Bell System Technical Journal*, vol. 27, no. 3, pp. 379–423, 1948.
- [2] D. Gündüz, D. B. Kurka, M. Jankowski, M. M. Amiri, E. Ozfatura, and S. Sreekumar, "Communicate to learn at the edge," *IEEE Communications Magazine*, vol. 58, no. 12, pp. 14–19, 2020.
- [3] M. Jankowski, D. Gündüz, and K. Mikolajczyk, "Deep joint source-channel coding for wireless image retrieval," in *IEEE International Conference on Acoustics, Speech and Signal Processing (ICASSP)*, 2020, pp. 5070–5074.
- [4] Y. Shao, D. Gündüz, and S. C. Liew, "Federated learning with misaligned over-the-air computation," *IEEE Trans. Wireless Commun.*, 2021.
- [5] Y. Shao, A. Rezaee, S. C. Liew, and V. W. S. Chan, "Significant sampling for shortest path routing: a deep reinforcement learning solution," *IEEE J. Sel. Areas Commun.*, vol. 38, no. 10, pp. 2234–2248, 2020.
- [6] V. Kostina, Y. Polyanskiy, and S. Verd, "Joint source-channel coding with feedback," *IEEE Transactions on Information Theory*, vol. 63, no. 6, pp. 3502–3515, 2017.
- [7] M. Gastpar, B. Rimoldi, and M. Vetterli, "To code, or not to code: Lossy source-channel communication revisited," *IEEE Transactions on Information Theory*, vol. 49, no. 5, pp. 1147–1158, 2003.
- [8] O. Orhan, D. Gunduz, and E. Erkip, "Source-channel coding under energy, delay, and buffer constraints," *IEEE Transactions on Wireless Communications*, vol. 14, no. 7, pp. 3836–3849, 2015.
- [9] G. Cheung and A. Zakhori, "Bit allocation for joint source/channel coding of scalable video," *IEEE Transactions on Image Processing*, vol. 9, no. 3, pp. 340–356, 2000.
- [10] E. Bourtsoulatz, D. B. Kurka, and D. Gündüz, "Deep joint source-channel coding for wireless image transmission," *IEEE Transactions on Cognitive Communications and Networking*, vol. 5, no. 3, pp. 567–579, 2019.
- [11] D. B. Kurka and D. Gündüz, "Deepjssc-f: Deep joint source-channel coding of images with feedback," *IEEE Journal on Selected Areas in Information Theory*, vol. 1, no. 1, pp. 178–193, 2020.
- [12] —, "Successive refinement of images with deep joint source-channel coding," in *2019 IEEE 20th International Workshop on Signal Processing Advances in Wireless Communications (SPAWC)*. IEEE, 2019, pp. 1–5.
- [13] M. Yang, C. Bian, and H.-S. Kim, "OFDM-guided deep joint source channel coding for wireless multipath fading channels," *IEEE Transactions on Cognitive Communications and Networking*, pp. 1–1, 2022.
- [14] K. Choi, K. Tatwawadi, A. Grover, T. Weissman, and S. Ermon, "Neural joint source-channel coding," in *International Conference on Machine Learning*. PMLR, 2019, pp. 1182–1192.
- [15] Y. M. Saidutta, A. Abdi, and F. Fekri, "Joint source-channel coding over additive noise analog channels using mixture of variational autoencoders," *IEEE Journal on Selected Areas in Communications*, vol. 39, no. 7, pp. 2000–2013, 2021.
- [16] E. Erdemir, P. L. Dragotti, and D. Gunduz, "Privacy-aware communication over the wiretap channel with generative networks," in *IEEE International Conference on Acoustics, Speech and Signal Processing (ICASSP)*, 2022.
- [17] T.-Y. Tung and D. Gündüz, "Deepwive: Deep-learning-aided wireless video transmission," *arXiv:2111.13034v1*, Nov. 2021.
- [18] D. B. Kurka and D. Gündüz, "Bandwidth-agile image transmission with deep joint source-channel coding," *IEEE Transactions on Wireless Communications*, vol. 20, no. 12, pp. 8081–8095, 2021.
- [19] J. Xu, B. Ai, W. Chen, A. Yang, P. Sun, and M. Rodrigues, "Wireless image transmission using deep source channel coding with attention modules," *IEEE Transactions on Circuits and Systems for Video Technology*, vol. 32, no. 4, pp. 2315–2328, 2022.
- [20] A. Krizhevsky, G. Hinton *et al.*, "Learning multiple layers of features from tiny images," University of Toronto, Tech. Rep., 2009.
- [21] D. Chu, "Polyphase codes with good periodic correlation properties (corresp.)," *IEEE Transactions on Information Theory*, vol. 18, no. 4, pp. 531–532, 1972.